Surface Roughness Effects on the Dynamic Characteristics of Finite Slider Bearings

Hsiu-Lu Chiang[*], Tsu-Liang Chou[*], Cheng-Hsing Hsu[**], Chia-Hao Hsu[**], and Jaw-Ren Lin[*]

[*] *Department of Mechanical Engineering, Nanya Institute of Technology*
[**] *Department of Mechanical Engineering, Chung Yuan Christian University*

ABSTRACT

The surface roughness effects on the dynamic characteristics of slider bearing with finite width are theoretically studied in this paper. Considering the transient motion of slider bearing and basing upon the Christensen's stochastic model, the dynamic stochastic Reynolds-type equation is derived. In order to study the dynamic characteristics, such as steady load-carrying capacity, dynamic stiffness and damping coefficients, small perturbation technique is applied. According to the results obtained, the performance characteristics of slider bearing are significant affected by the roughness pattern, the profile parameter and the width-to-length ratio. As a result, the steady load-carrying capacity, dynamic stiffness and damping coefficient are increased as the effects of transverse roughness increase. On the other hand, the influences of the isotropic and longitudinal roughness have a reverse trend. On a whole, as the values of roughness parameter increase, the effects of surface roughness on the bearing load, the stiffness and damping coefficients increase.

Keywords: Christensen's stochastic model, surface roughness, slider bearings, dynamic coefficient

表面粗糙度對有限長滑塊軸承的動態特性效應

江新祿[*] 周祖亮[*] 許政行[**] 許家豪[**] 林昭仁[*]

[*] 南亞技術學院 機械工程系
[**] 中原大學 機械工程學系

摘 要

本研究在探討有限長滑塊軸承受到表面粗糙度影響時，系統的動態係數特性。根據Christensen的隨機模式，吾人可推導出考慮滑塊暫態運動時的動態隨機雷諾方程式。應用小波擾動理論，系統穩態負載能力和動態剛性及阻尼係數便可預測。根據研究所得結果，粗糙度型式、滑塊輪廓參數和長寬比對軸承特性有顯著之影響。研究亦顯示，橫向粗糙度可增加系統的負載能力、動態剛性係數與阻尼係數；然而，均勻等向和縱向粗糙度對軸承特性的影響恰好相反。總而言之，增加粗糙度參數值可增加表面粗糙度對軸承負荷、剛性和阻尼係數的影響。

關鍵詞： Christensen 隨機模式，表面粗糙度，滑塊軸承，動態係數

文稿收件日期 92.7.2; 文稿修正後接受日期 94.8.9
Manuscript received July 2,2003; revised Aug. 9, 2005

I. INTRODUCTION

Sliding bearings, in engineering application, are used as the transverse-load sustainer and, being amenable to easy mathematical analysis, there are many studies investigated for various film shapes [1, 2]. In practice, it is well known that bearing surfaces made by various forming processes and after some run-in and wear, they are not perfectly smooth and some asperities maybe exist. In other cases, the contamination of lubricant is also capable of making the bearing surface rough through chemical degradation. Moreover, when the roughness is about the same order of magnitude as the film thickness, the effect of surface asperities becomes important. In order to simulate theoretically the effect of surface asperity, the random character of the surface roughness using the stochastic concept, was proposed by Christensen and Tonder [3, 4]. In Christensen's stochastic model with an approximate probability density function, an overall analysis both for one-dimensional longitudinal and transverse roughness types along with two-dimensional isotropic roughness is explored.

Plenty of studies investigated in the effects of the surface roughness on the performance characteristics of slider bearings have been submitted past the decades. Phan-Thien and Atkinson [5] discussed the effects of homogeneous Reynolds roughness in slider bearing with exponential film thickness, pointing out the application criterion of the Reynolds equation. Thereafter, the rheological aspects of lubricant and surface roughness effect on the load-carrying capacity of slider bearing are studied by Wang [6], and the dynamic effects of a sliding train with transversely oriented undulations on rectangular bearings are studied by Tonder [7]. Recently, the effects of surface roughness on the performance of hydrodynamic slider bearings are explored by Andharia et al. [8], and the average grain flow lubrication of finite-width slider bearing is numerically solved by Jeng and Tsai [9]. All abovementioned researches, even though, were confined in the region of steady state and the dynamic stability characteristics of the system, meanwhile, are not consider

It is conceived, though, that the steady-state characteristics should be taken into consideration during bearing designing; nevertheless, the dynamic performances of the system cannot be overlooked. Contacts between slider bearing and pad maybe occur due to poor dynamic performances and can endanger the safety operation of the system. Since the surfaces of slider bearing run primarily on the wedge-action, so, understanding of dynamic stiffness and damping behaviors is needed and necessary; thus, a further and thorough study of the dynamic squeezing effects is required. In the previous works of authors, the linear stability analysis of a wide inclined plane (one-dimensional) [10] and slider bearing with finite width (two-dimensional) [11] were analyzed; but for simplicity, the surface roughness effects on the performance features of slider bearing are not considered yet.

The purpose of this study is to explore the effects of surface roughness on the dynamic characteristics of an inclined slider bearing with finite width. During the derivation of generalized dynamic stochastic Reynolds equation for a finite width bearing, the transient motion of the slider is also considered. When applying the linear perturbation method, the two dimensional Reynolds-type equation, taking the squeezing wedge-action effect of the bearing into account, is perturbed into two equations, one responsible for steady-state performance and the other the dynamic characteristics, respectively. At last, as the pressure distributions of the lubricant were known, the load-carrying capacity, dynamic stiffness and damping coefficients can be evaluated for various profile parameter, width-to-length ratio and roughness parameter with different types of surface roughness.

II. FORMULATION

The physical configuration of squeeze-film bearing with finite width B and length L is sketched in figure 1. As traditionally, the thin film lubrication theory is applied and the flow being assumes incompressible, laminar and isothermal. Extending the previous work [10, 11], the generalized Reynolds-type equation is obtained.

$$\frac{\partial}{\partial x}(H^3\frac{\partial p}{\partial x})+\frac{\partial}{\partial y}(H^3\frac{\partial p}{\partial y})=6\mu U\frac{\partial H}{\partial x}+12\mu\frac{\partial H}{\partial t} \tag{1}$$

In equation (1), variables H and p denote the local film thickness and film pressure, respectively; while x and y depict the rectangular coordinate on the horizontal plane, U the sliding velocity of lower surface, μ the viscosity of lubricant and, t is time. As shown in Fig.1, the local film thickness H can be considered made up of two parts:

$$H=h_s(x)+h_m(t)=d(1-\frac{x}{L})+h_m(t) \tag{2}$$

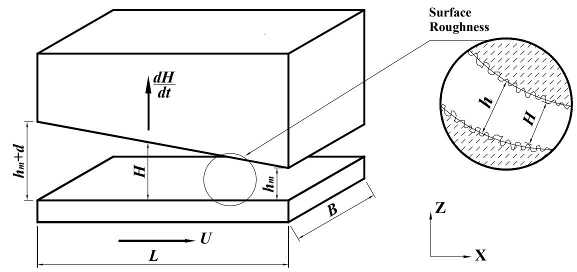

Fig.1. Configuration of a journal bearing.

where $h_s(x)$ is the slider profile already known and $h_m(t)$ the minimum film thickness depending only on the squeezing time t.

2.1 Stochastic Reynolds Equation

Following Christensen's stochastic surface roughness Model [3-4] and taking expected values of system governing equation (1), the generalized stochastic Reynolds-type equation can be obtained:

$$\frac{\partial}{\partial x}E(H^3\frac{\partial p}{\partial x})+\frac{\partial}{\partial y}E(H^3\frac{\partial p}{\partial y})=6\mu U\frac{\partial}{\partial x}E(H)+12\mu\frac{\partial}{\partial t}E(H) \tag{3}$$

where $E(\cdot)$ denotes the expectancy operator defined by：

$$E(\cdot)=\int_{-\infty}^{\infty}(\cdot)f(\nu)d\nu \tag{4}$$

and f is the probability density distribution for the stochastic variable. Since most of the engineering surface roughness is found to be Gaussian height distribution in nature; so, a polynomial function approximate to the Gaussian distribution is chosen for simplicity.

$$f(\nu)=\begin{cases}\dfrac{35}{32c^7}(c^2-\nu^2)^3 & \text{if } -c\le\nu\le c\\ 0 & \text{elsewhere}\end{cases} \tag{5}$$

In equation (5), c is one half the total range of the random film thickness variable, while $\nu(x,y,\xi)$ is the part due to the surface asperities measured from the nominal level and is regarded as a randomly varying quantity of zero mean. The function terminates at $c=3\sigma$, where σ is the standard deviation. Three types of roughness structure, the avowed one-dimensional longitudinal and transverse roughness as well as the two-dimensional isotropic roughness pattern, are of interest in present study.

For one-dimensional longitudinal roughness, the structure has the form of long narrow ridge and valleys running in the x direction. Under such situation, the local film thickness H is

$$H=h(x,t)+\nu(y,\xi) \tag{6}$$

where $h(x,t)=h_s(x)+h_m(t)$ and the stochastic Reynolds-type equation can be expressed as

$$\frac{\partial}{\partial x}\left[E(H^3)\frac{\partial\bar{p}}{\partial x}\right]+\frac{\partial}{\partial y}\left[E(\frac{1}{H^3})\frac{\partial\bar{p}}{\partial y}\right] = 6\mu U\frac{\partial}{\partial x}E(H)+12\mu\frac{\partial}{\partial t}E(H) \tag{7}$$

For transverse one-dimensional roughness, the surface has the form of long narrow ridge and valleys running in the y direction. In this case, the local film thickness H is

$$H=h(x,t)+\nu(x,\xi) \tag{8}$$

and the stochastic Reynolds-type equation can be expressed as

$$\frac{\partial}{\partial x}\left[E(\frac{1}{H^3})\frac{\partial\bar{p}}{\partial x}\right]+\frac{\partial}{\partial y}\left[E(H^3)\frac{\partial\bar{p}}{\partial y}\right] = 6\mu U\frac{\partial}{\partial x}\frac{E\left(1/H^2\right)}{E\left(1/H^3\right)}+12\mu\frac{\partial}{\partial t}E(H) \tag{9}$$

For isotropic roughness structure, the roughness is assumed uniformly distributed over the bearing surface with no preferred direction, and the local film thickness H is

$$H=h(x,t)+\nu(x,y,\xi) \tag{10}$$

and the stochastic Reynolds-type equation can be expressed as

$$\frac{\partial}{\partial x}\left[E(H^3)\frac{\partial\bar{p}}{\partial x}\right]+\frac{\partial}{\partial y}\left[E(H^3)\frac{\partial\bar{p}}{\partial y}\right] = 6\mu U\frac{\partial E(H)}{\partial x}+12\mu\frac{\partial E(H)}{\partial t} \tag{11}$$

wher $\bar{p}=E(p)$ is the mean hydrodynamic pressure. If one substitutes corresponding degrees of local film thickness H into Gaussian expectancy operator $E(\cdot)$ and the higher order terms being truncated, one has the following approximate relationships:

$$E(H)\approx h$$
$$E\left(H^3\right)\approx h^3+\frac{1}{3}hc^2 \tag{12}$$
$$E(\frac{1}{H^3})\approx h^3-\frac{2}{3}hc^2$$

To simplify the procedure of numerical analysis, one can define the following dimensionless parameters:

$$p^*=\frac{ph_{mo}^2}{\mu UL},\quad x^*=\frac{x}{L},\quad y^*=\frac{y}{B},\quad \tau=\frac{Ut}{L},$$
$$\beta=\frac{B}{L},\quad \delta=\frac{d}{h_{m0}},\quad \Lambda=\frac{c}{h_{m0}},\quad h^*=\frac{h}{h_{m0}} \tag{13}$$

where β , Λ an δ are parameters of width-to-length ratio, roughness and profile, respectively. After some manipulations, the dimensionless local film thickness and generalized stochastic Reynolds-type equations can be derived:

$$h^*(x^*,\tau)=h_s^*(x^*)+h_m^*(\tau)=\delta(1-x^*)+h_m^*(\tau) \tag{14}$$

$$\frac{\partial}{\partial x^*}\left[F^*(h^*,\Lambda)\frac{\partial \overline{p}^*}{\partial x^*}\right]+\frac{1}{\beta^2}\frac{\partial}{\partial y^*}\left[G^*(h^*,\Lambda)\frac{\partial \overline{p}^*}{\partial y^*}\right]=6\frac{\partial h_R^*(h^*,\Lambda)}{\partial x^*}+12\frac{\partial h^*}{\partial \tau} \tag{15}$$

where

$$F^*(h^*,\Lambda)=\begin{cases} h^{*3}+\frac{1}{3}h^*\Lambda^2 & \text{longitudinal roughness}\\ h^{*3}-\frac{2}{3}h^*\Lambda^2 & \text{transverse roughness}\\ h^{*3}+\frac{1}{3}h^*\Lambda^2 & \text{isotropic roughness}\end{cases}$$

$$G^*(h^*,\Lambda)=\begin{cases} h^{*3}-\frac{2}{3}h^*\Lambda^2 & \text{longitudinal roughness}\\ h^{*3}+\frac{1}{3}h^*\Lambda^2 & \text{transverse roughness}\\ h^{*3}+\frac{1}{3}h^*\Lambda^2 & \text{isotropic roughness}\end{cases} \tag{16}$$

$$h_R^*(h^*,\Lambda)=\begin{cases} h^* & \text{longitudinal roughness}\\ h^*-\frac{1}{3}\frac{\Lambda^2}{h^*} & \text{transverse roughness}\\ h^* & \text{isotropic roughness}\end{cases}$$

If small perturbation technique is applied, the minimum film thickness and the local mean film pressure are perturbed as following:

$$h_m^*=1+\varepsilon\, e^{i\tau} \tag{17}$$

$$\overline{p}^*=\overline{p}_0^*+\overline{p}_1^*\varepsilon\, e^{i\tau} \tag{18}$$

where ε represents the small perturbed amplitude and $i=\sqrt{-1}$. Substituting equations (17-18) into the generalized stochastic Reynolds-type equation (15) and the high order terms being neglected, one can obtain Reynolds equations responsible for the steady state and dynamic state characteristics at the meanwhile.

2.2 Steady-state characteristics

$$\frac{\partial}{\partial x^*}\left[f^*(h_s^*,\Lambda)\frac{\partial \overline{p}_0^*}{\partial x^*}\right]+\frac{1}{\beta^2}\frac{\partial}{\partial y^*}\left[g^*(h_s^*,\Lambda)\frac{\partial \overline{p}_0^*}{\partial y^*}\right]=6\frac{\partial h_s^*}{\partial x^*}+\frac{\partial}{\partial x^*}m^*(h_s^*,\Lambda) \tag{19}$$

where

$$f^*(h_s^*,\Lambda)=\begin{cases} (h_s^*+1)^3+\frac{1}{3}\Lambda^2(h_s^*+1) & \text{longitudinal roughness}\\ (h_s^*+1)^3-\frac{2}{3}\Lambda^2(h_s^*+1) & \text{transverse roughness}\\ (h_s^*+1)^3+\frac{1}{3}\Lambda^2(h_s^*+1) & \text{isotropic roughness}\end{cases}$$

$$g^*(h_s^*,\Lambda)=\begin{cases} (h_s^*+1)^3-\frac{2}{3}\Lambda^2(h_s^*+1) & \text{longitudinal roughness}\\ (h_s^*+1)^3+\frac{1}{3}\Lambda^2(h_s^*+1) & \text{transverse roughness}\\ (h_s^*+1)^3+\frac{1}{3}\Lambda^2(h_s^*+1) & \text{isotropic roughness}\end{cases} \tag{20}$$

$$m(h_s^*,\Lambda)=\begin{cases} 0 & \text{longitudinal roughness}\\ -\frac{2\Lambda^2}{h_s^*+1} & \text{transverse roughness}\\ 0 & \text{isotropic roughness}\end{cases}$$

2.3 Dynamic-state characteristics

$$\begin{aligned}&\frac{\partial}{\partial x^*}\left[f^*(h_s^*,\Lambda)\frac{\partial \overline{p}_1^*}{\partial x^*}\varepsilon\, e^{i\tau}\right]+\frac{1}{\beta^2}\frac{\partial}{\partial y^*}\left[g^*(h_s^*,\Lambda)\frac{\partial \overline{p}_1^*}{\partial y^*}\varepsilon\, e^{i\tau}\right]\\ &=12i\varepsilon\, e^{i\tau}+\frac{1}{2\Lambda^2}\frac{\partial}{\partial x^*}\left[m^{*2}(h_s^*,\Lambda)\varepsilon\, e^{i\tau}\right]\\ &-\frac{\partial}{\partial x^*}\left[s^*(h_s^*,\Lambda)\frac{\partial \overline{p}_0^*}{\partial x^*}\varepsilon\, e^{i\tau}\right]-\frac{1}{\beta^2}\frac{\partial}{\partial y^*}\left[T^*(h_s^*,\Lambda)\frac{\partial \overline{p}_0^*}{\partial y^*}\varepsilon\, e^{i\tau}\right]\end{aligned} \tag{21}$$

where

$$s^*(h_s^*,\Lambda)=\begin{cases} 3(h_s^*+1)^2+\frac{1}{3}\Lambda^2 & \text{longitudinal roughness}\\ 3(h_s^*+1)^2-\frac{2}{3}\Lambda^2 & \text{transverse roughness}\\ 3(h_s^*+1)^2+\frac{1}{3}\Lambda^2 & \text{isotropic roughness}\end{cases}$$

$$T^*(h_s^*,\Lambda)=\begin{cases}3(h_s^*+1)^2-\dfrac{2}{3}\Lambda^2 & \text{longitudinal roughness}\\ 3(h_s^*+1)^2+\dfrac{1}{3}\Lambda^2 & \text{transverse roughness}\\ 3(h_s^*+1)^2+\dfrac{1}{3}\Lambda^2 & \text{isotropic roughness}\end{cases} \quad (22)$$

The boundary conditions of the system for the mean steady and dynamic film pressure $\overline{p}_0^*$ and $\overline{p}_1^*$ are

$$\begin{cases}\overline{p}_0^*=0 \quad x^*=0,1 \text{ and } y^*=0,1\\ \overline{p}_1^*=0 \quad x^*=0,1 \text{ and } y^*=0,1\end{cases} \quad (23)$$

III. BEARING CHARACTERISTICS

Though equations (19) and (21) are, being responsible for steady state and dynamic state characteristics respectively, highly non-linear and cannot be solved theoretically, but they are possible to be calculated numerically using the method of Precondition Conjugate Gradient (PCGM) [12]. The finite difference forms of the stochastic Reynolds-type equation are

$$a_0p_{0i,j}^*+a_1p_{0i+1,j}^*+a_2p_{0i-1,j}^*+a_3p_{0i,j+1}^*+a_4p_{0i,j-1}^*=B_{ij} \quad (24)$$

$$\begin{aligned}&a_0p_{1i,j}^*+a_1p_{1i+1,j}^*+a_2p_{1i-1,j}^*+a_3p_{1i,j+1}^*+a_4p_{1i,j-1}^*\\&=b_0+b_1p_{0i,j}^*+b_2p_{0i+1,j}^*+b_3p_{0i-1,j}^*+b_4p_{0i,j+1}^*+b_5p_{0i,j-1}^*\end{aligned} \quad (25)$$

where $p_{0i,j}^*$ and $p_{1i,j}^*$ denote the dimensionless steady and dynamic pressures at the grid point (i, j) respectively, and the coefficients in equations (24-25) are defined as following:

$$\begin{aligned}a_0&=-\beta^2r^{*2}\left(f_{i+1/2,j}^*+f_{i-1/2,j}^*\right)-\left(g_{i,j+1/2}^*+g_{i,j-1/2}^*\right)\\ a_1&=\beta^2r^{*2}f_{i+1/2,j}^*\\ a_2&=\beta^2r^{*2}f_{i-1/2,j}^*\\ a_3&=g_{i,j+1/2}^*\\ a_4&=g_{i,j-1/2}^*\\ B_{ij}&=\delta\,\beta^2(\Delta y^*)^2[-6+\hat{m}_{ij}(h_s^*,\Lambda)]\end{aligned} \quad (26)$$

$$\hat{m}_{ij}(h_s^*,\Lambda)=\begin{cases}0 & \text{longitudinal roughness}\\ -\dfrac{2\Lambda^2}{[(h_s^*)_{i,j}+1]^2} & \text{transverse roughness}\\ 0 & \text{isotropic roughness}\end{cases}$$

$$\begin{aligned}r^{*2}&=\left(\Delta y^*/\Delta x^*\right)^2\\ b_0&=12i\beta^2(\Delta y^*)^2\,\varepsilon\,e^{i\tau}+b_R\\ b_1&=\beta^2r^{*2}\left(s_{i+1/2,j}^*+s_{i-1/2,j}^*\right)\varepsilon\,e^{i\tau}-\left(T_{i,j+1/2}^*+T_{i,j-1/2}^*\right)\,\varepsilon\,e^{i\tau}\\ b_2&=-\beta^2r^{*2}s_{i+1/2,j}^*\varepsilon\,e^{i\tau}\\ b_3&=-\beta^2r^{*2}s_{i-1/2,j}^*\varepsilon\,e^{i\tau}\\ b_4&=-T_{i,j+1/2}^*\varepsilon\,e^{i\tau}\\ b_5&=-T_{i,j-1/2}^*\varepsilon\,e^{i\tau}\end{aligned} \quad (27)$$

$$b_R=\begin{cases}0 & \text{longitudinal roughness}\\ \delta\,\beta^2(\Delta y^*)^2\dfrac{4\Lambda^2}{[(h_s^*)_{i,j}]^3}\varepsilon\,e^{i\tau} & \text{transverse roughness}\\ 0 & \text{isotropic roughness}\end{cases}$$

The steady state film pressure $\overline{p}_0^*$ and perturbed film pressure $\overline{p}_1^*$ can be calculated iteratively from equations (24-25) using PCGM method until the accuracy meets the following criteria:

$$\left|\frac{\overline{p}_{0i,j}^{*\,(k+1)}-\overline{p}_{0i,j}^{*\,(k)}}{\overline{p}_{0i,j}^{*\,(k)}}\right|<0.0001 \quad (28)$$

$$\left|\frac{\overline{p}_{1i,j}^{*\,(k+1)}-\overline{p}_{1i,j}^{*\,(k)}}{\overline{p}_{1i,j}^{*\,(k)}}\right|<0.0001 \quad (29)$$

where $\overline{p}_{0\,i,j}^{*\,(k)}$ represents the k-th iterative value of $\overline{p}_{0\,i,j}^*$

Once the mean steady and dynamic film pressures are obtained, the steady load capacity W_0^* and the perturbed film force W_1^* can be calculated by integrating the steady pressure and the perturbed pressure over the whole film region respectively.

$$W_0^* = \frac{W_0 h_{m0}^2}{\mu U L^2 B} = \int_{x^*=0}^{x^*=1}\int_{y^*=0}^{y^*=1} \overline{p}_0^* dx^* dy^* \quad (30)$$

$$W_1^* = \frac{W_1 h_{m0}^2}{\mu U L^2 B} = \int_{x^*=0}^{x^*=1}\int_{y^*=0}^{y^*=1} \overline{p}_1^* dx^* dy^* \quad (31)$$

On the basis of the small linear perturbation theory, the perturbed film load W_1 can be written in terms of stiffness coefficient K, the real part, and damping coefficient D, the imaginary part, as

$$W_1 \varepsilon\, e^{i\tau} = -K h_{m0} \varepsilon\, e^{i\tau} - D \frac{d\left(h_{m0}\varepsilon\, e^{i\tau}\right)}{d\tau} \quad (32)$$

or simply after cancellation of the same term and expressed in dimensionless forms as

$$W_1^* = -K^* - iD^* \quad (33)$$

Then, the stiffness and damping coefficients can be derived, comparing equation (31) with equation (33), from the real and imaginary part of the perturbed film load W_1^* as

$$K^* = \frac{K h_{m0}^3}{\mu U L^2 B} = -\mathrm{Re}\left(W_1^*\right) = -\sum_{i=0}^{m}\sum_{j=0}^{n} \mathrm{Re}\left(\overline{p}_1^*\right)_{i,j} \Delta x^* \Delta y^* \quad (34)$$

$$D^* = \frac{D h_{m0}^3}{\mu L^3 B} = -\mathrm{Im}\left(W_1^*\right) = -\sum_{i=0}^{m}\sum_{j=0}^{n} \mathrm{Im}\left(\overline{p}_1^*\right)_{i,j} \Delta x^* \Delta y^* \quad (35)$$

IV. RESULTS AND DISCUSSIONS

Applying the Christensen's stochastic model, the transient squeezing actions with roughness effect on the performance characteristics of two-dimensional finite slider bearing are investigated, where the surface roughness effect is characterized by roughness parameter defined as $\Lambda = c/h_{m0}$. If the value of Λ approaches zero, the performance characteristics of the system behave as a smooth bearing. The dynamic behaviors are studied by using a first order perturbation method with small oscillations and the steady state solution and dynamic coefficients are predicted for various profile parameter, width-to-length ratio and roughness parameter.

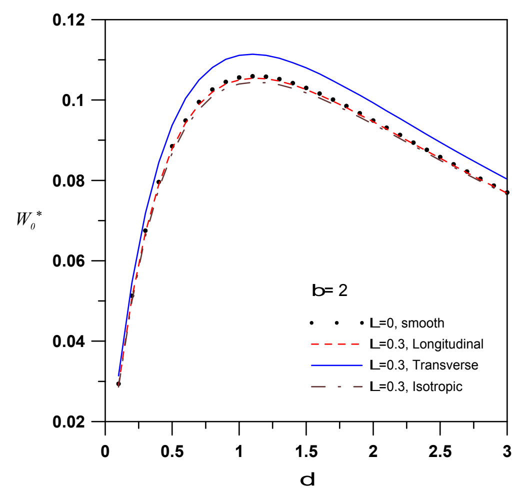

Fig. 2. Dimensionless steady load capacity W_0^* versus profile parameter δ .

The variation of the dimensionless steady load-carrying capacity versus the profile parameter δ is depicted in Fig. 2. For bearings with finite width β =2, it is seen that, as the profile parameter increases, the load-carrying capacity increases sharply first until a critical maximum value reaches (δ =1), and increases the profile parameter further, the value of W_0^* decreases gradually. The extending numerical simulation acquired in this study agrees very well as compared with that of smooth case obtained by Lin et al. [10] or Lu and Lin [11], and this assured the correctness of the stochastic roughness model adopted presently. As the roughness effect on the steady load- carrying capacity, in contrast with the smooth case, it is shown that the effect of the transverse roughness has an enhancement of load-carrying capacity, especially for larger profile parameter.

On the contrary, the influences of longitudinal and isotropic roughness reduce the values, but the difference is marginal. The relationship between ratio of width-to-length β and load capacity can be inspected in Fig. 3. Obviously, the increment of load capacity is splendor when $\beta<10$, but the improvement is slight as the ratio β is higher than 10. The tendency of the roughness effect on the variation of load capacity is similar between ratio β and profile parameter δ ; *i.e.*, the load capacity of transverse roughness case is higher than that of smooth bearing, while the longitudinal and isotropic roughness cases have the reverse trend, but the quantity of decrement is not distinct when $\beta<5$.

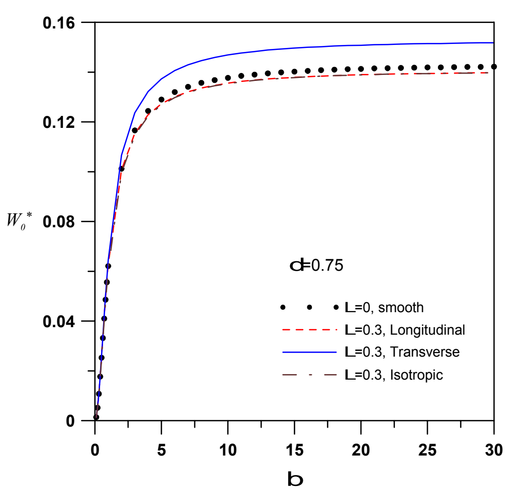

Fig. 3. Effect of the variation of width-to-length ratio β on the steady load capacity W_0^*.

The variations of load-carrying capacity versus roughness parameter Λ are depicted in Fig. 4. It is obviously that load-carrying capacity greatly enhances in transverse roughness type as the roughness parameter increases; especially, the improvement is dominant as the slider bearing possesses a rougher surface. Additionally, the effect of isotropic roughness is to lower down the bearing load. On the other way, the affection of longitudinal roughness to load-carrying capacity is insignificant and marginal and can be neglected. On a whole, the effect for different surface roughness type caused by surface texture on the characteristics of load-carrying capacity is very distinct, and these changes are induced by the alteration of the flow direction due to the presence of surface roughness.

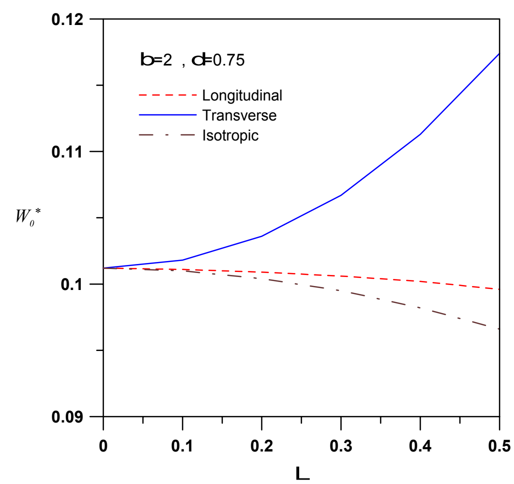

Fig. 4. Variation of dimensionless steady load capacity W_0^* w. r. t. roughness parameter Λ .

Relationships between dynamic behaviors and profile parameter δ are plotted in Fig. 5. As shown in the figure, there exists a critical value of profile parameter ($\delta=0.6$) such that the dynamic stiffness K^* has a maximum. On the contrary, the dynamic damping coefficient D^* monotonically decreases as increasing profile value. When the influence of surface roughness is taken into apart, the influence of one-dimensional transverse roughness improves values of K^* and D^*, whereas the other two types of surface roughness have little significance in the action of dynamic coefficients as comparing to the smoothing case. A further insight into this dynamic performance can be observed in Fig. 6. As demonstrated, the quantities of dynamic stiffness and damping coefficients enhance quickly for the ratio of width-to-length β increases till 10. As expected, when compared to the results of smooth case, the transverse roughness effect promotes the values of dynamic coefficients, while surface with isotropic asperity or longitudinal roughness have the reverse trend.

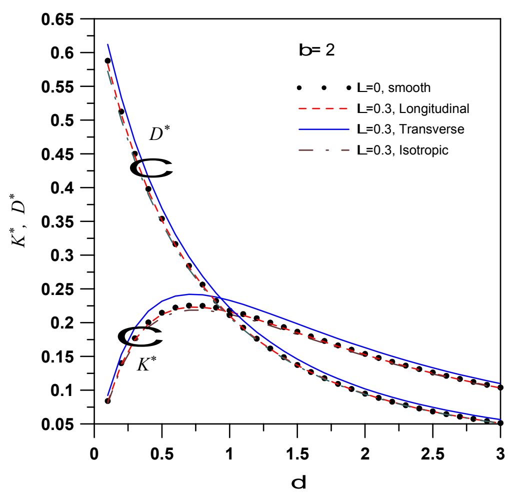

Fig. 5. Dimensionless dynamic coefficient K^* and D^* versus profile parameter δ.

In Fig. 7, the variation of dynamic coefficients with roughness parameter Λ is illustrated. Apparently, the surface working structure is important during bearing design. If the surface roughness model is varied, the effect on the dynamic coefficients could be completely reverse. In present study, it is found out that, the larger the roughness parameter is, the higher the values of dynamic stiffness and damping coefficients obtain in the transverse roughness case, while the effect of isotropic asperity has the reverse tendency. On a whole, better dynamic performance characteristics are predicted in a smaller inclination or a wider slider bearing possessed with a transverse-roughness type manufacture process.

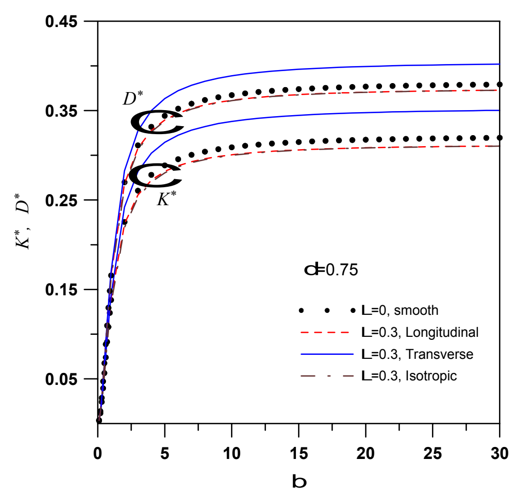

Fig. 6. Effect of the variation of β on the dynamic coefficient K^* and D^*.

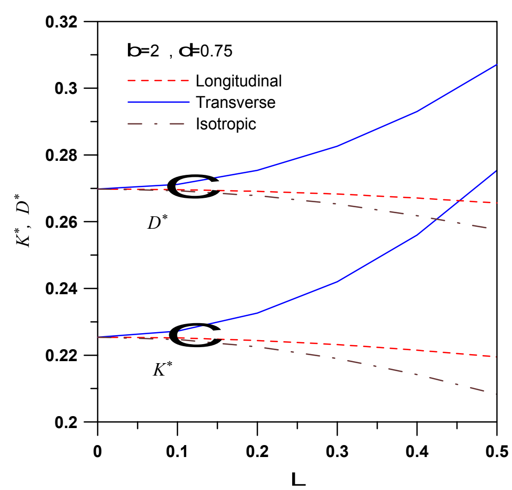

Fig. 7. Variation of dynamic coefficient K^* and D^* w. r. t. roughness parameter Λ.

V. CONCLUSION

On the basis of the Christensen's stochastic model, the influence of the surface roughness on a slider bearing with finite width is studied. Taking into account the transient motion of the slider, the dynamic stochastic Reynolds-type equation is derived to explain the surface asperity made by various machining and polishing process. Using the small perturbation technique, the steady load-carrying capacity as well as dynamic stiffness and damping coefficients are predicted. According to the theoretical analysis, one has:

1. The roughness pattern, profile parameter and width-to-length ratio of the bearing have significant effects upon the bearing characteristics.
2. As the slider bearing is determined, there exists a critical value of profile parameter such that the load-carrying capacity and dynamic stiffness coefficient of the system are maximal. Meanwhile, the larger the width-to-length ratio one has the higher load capacity the system can sustain.
3. In contrast to the smooth bearing, the effect of one-dimensional transverse roughness can enhance load-carrying capacity and dynamic coefficients of the system, especially at a higher surface roughness parameter or width-to-length ratio. The influences of longitudinal and isotropic roughness on the lubricant performance characteristics have the reverse trend.
4. A smaller profile parameter or a wider slider bearing with a transverse roughness type gives the better dynamic stiffness and damping coefficients.

NOMENCLATURE

B	bearing width
c	one half the total range of the random film thickness variable
d	slider height difference
$D,\ D^*$	dimension and dimensionless damping coefficient
$E(\cdot)$	expectancy operator
f	probability density distribution for the stochastic variable
$h_s(x)$	known slider profile
$h_m(t)$	minimum squeezed film thickness
h_{m0}	steady state minimum squeezed film thickness
H	local film thickness
$K,\ K^*$	dimension and dimensionless stiffness coefficient
L	bearing length
P	local film pressure
$\bar{p}, \bar{p}^*$	mean squeezed film pressure
$\bar{P}_0^*$	mean steady film pressure
$\bar{P}_1^*$	mean dynamic film pressure
t	time
W_0, W_1	steady and dynamic load capacity
W_0^*, W_1^*	dimensionless steady and dynamic load capacity
x, y	rectangular coordinates
x^*, y^*	dimensionless coordinates
β	width-to-length ratio
δ	profile parameter
ε	small perturbed amplitude
Λ	roughness parameter
μ	lubricant shear viscosity
ν	random part of film geometry
σ	standard deviation
τ	dimensionless time

REFERENCES

[1] Pinkus, O. and Sternlitcht, B., Theory of Hydrodynamic Lubrication, McGraw Hill, New York, 1961.

[2] Hamrock, B. J., Fundamentals of Fluid Film Lubrication, McGraw Hill, New York, 1994.

[3] Christensen, H., "Stochastic Models for Hydrodynamic Lubrication of Rough Surfaces," J. Proc. Instn. Mech. Engrs., Vol. 184, pp. 1013-1026, 1969-70.

[4] Christensen, H., and Tonder, K., "The Hydrodynamic Lubrication of Rough Bearing Surfaces of Finite Width," J. Lubr. Tech., Vol. 93, pp. 324-330, 1971.

[5] Phan-Thien, N., and Atkinson, A. D., "On the Effects of Homogeneous Reynolds Roughness in a Two-dimensional Slider Bearing with Exponential Film Thickness," Transaction of ASME, Vol. 104, pp. 220-226, 1982.

[6] Wang, J., "The Effects of Rheological Characteristics of Lubricant and Surface Roughness on the Load Capacity of a Hydrodynamic Slider Bearing," Wear, Vol. 146, pp. 165-177, 1991.

[7] Tonder, K., "Dynamics of Rough Slider Bearings: Effects of One-sided Roughness/ Waviness," Tribol. Int., Vol. 29, No. 2, pp. 117-122, 1996.

[8] Andharia, P. I., Gupta, J. L., and Deheri, G. M., "Effect of Surface Roughness on Hydrodynamic Lubrication of Slider Bearings," Tribol. Trans., Vol. 44, No. 2, pp. 291-297, 2001.

[9] Jeng, Y. R., and Tsai, H. J., "Grain-flow Lubrication of Finite-width Slider Bearing with Rough Surface," Tribol. Letters, Vol. 13, No. 4, pp. 219-232, 2002.

[10] Lin, J. R., Lu, R. F., and Yang, C. B., "Linear Stability Analysis of a Wide Inclined Plane Slider Bearing," J. Sci. and Techno., Vol. 10, No. 5, pp. 349-354, 2001.

[11] Lu, R. F. and Lin, J. R., "Linear Stability Analysis of Finite Slider Bearings," J. Sci. and Techno., Vol. 11, No. 5, pp. 341-347, 2002.

[12] Burden, R. L. and Fairs, J. D., Numerical Analysis, Brooks/Cole Publishing Company, Pacific Grove, 2001.